Clinics in Surgery

Research Article
Published: 28 Jun, 2018

The Mechanism of Bacterial Translocation after Major Hepatectomy in Cirrhotic Rats

*Jian Liang[1,2], Zhi-qiang Ye[3], Shu-xian Chen[1], Chu-si Wan[1] and Wei-dong Pan[1]**

[1]Department of Hepatopancreatobiliary Surgery, The Third Affiliated Hospital of Sun Yat-sen University, China

[2]Department of General Surgery, Hospital of Traditional Chinese Medicine of Zhongshan, China

[3]Department of Emergency, The Third Affiliated Hospital of Sun Yat-sen University, China

Abstract

This study was designed to investigate the mechanism underlying bacterial translocation after major hepatectomy in cirrhotic rats. Sixty experimental cirrhotic rats were randomly divided into SO, PH and PHP groups. Portal pressure, the composition of the intestinal micro flora, the levels of D-lactic acid, endo toxins, inflammatory factors, and tight junction proteins were analyzed in the three groups of animal. Portal pressure of the PH rats was significantly higher (22.48 ± 0.882 cm H2O) than that of the SO (14.3 ± 1.25 cm H2O) and PHP rats (16.6 ± 1.02 cm H2O) (P<0.05). The PH rats also showed significantly higher levels of serum LPS and D-lactic acid (52.56 ± 2.08 EU/ml and 60.87 ± 4.44 mg/L) than the SO (48.28 ± 1.45 EU/ml and 37.23 ± 1.71 mg/L) and PHP rats (47.84 ± 3.45 EU/ml and 40.83 ± 1.82 mg/L) (P<0.05). ZO-1 and Claudin-1 levels were significantly higher in the SO and PHP rats than in the PH rats (P<0.05), and the expression levels of TNF-α, IFN-γ, and MLCK were significantly lower in the SO and PHP rats than in the PH rats (P<0.05). Portal pressure significantly increased after major hepatectomy in cirrhotic rats, leading to intestinal stagnant anoxia, the accumulation of local metabolic products and inflammatory factors, the induction of intestinal epithelial cell apoptosis, and changes in the composition of the gut flora. These effects collectively resulted in tight junction functional disorders.

Keywords: Cirrhosis; Major hepatectomy; Bacterial translocation; Gut barrier

OPEN ACCESS

Correspondence:
Wei-dong Pan, Department of Hepatopancreatobiliary Surgery, The Third Affiliated Hospital of Sun Yat-sen University, China, Tel: +86-20-85253178; Fax: +86-20-85253336; E-mail: panwd@mail.sysu.edu.cn

Received Date: *07 Jun 2018*
Accepted Date: *21 Jun 2018*
Published Date: *28 Jun 2018*

Citation:
Liang J, Ye Z-q, Chen S-x, Wan C-s, Pan W-d. The Mechanism of Bacterial Translocation after Major Hepatectomy in Cirrhotic Rats. Clin Surg. 2018; 3: 2002.

Introduction

Postoperative infection is a common complication of major hepatectomy, after which it represents an important cause of patient deaths [1]. Studies have shown that postoperative infection following major hepatectomy is closely associated with intestinal Bacterial Translocation (BT) [2,3] and leads to increased mortality. The reasons that these endogenous infections occur remain elusive, and no single determinant has been recognized. Studies have shown that portal venous pressure sharply increases during major hepatectomy and that portal hypertension can lead to congestion and edema of the bowel intestinal barrier. These changes may enable the translocation of intestinal tract bacteria from the intestinal lumen to tissues and organs in the abdominal cavity, where they can stimulate a series of inflammatory responses [3]. Determining the mechanism underlying BT and identifying ways to maintain the integrity of the intestinal barrier are therefore important goals for research on major hepatectomy. In the present study, we investigated the changes that occurred in the mechanical and bacterial barriers of the intestines of cirrhotic rats that underwent major hepatectomy with the goal of identifying the mechanisms underlying bacterial translocation.

Materials and Methods

Experimental animals

In the present study, the Specific Pathogen-Free (SPF) levels of 80 male Sprague Dawley (SD) rats weighing 80 g to 100 g were measured. The rats were purchased from the animal experimental center of Sun Yat-sen University and fed at the animal experimental center of Sun Yat-sen University, North Campus, in a SPF-level barrier environment (experimental animal usage license No. SYXK (Guangdong 2012-0081). The rats were fed under artificial lighting every 12 hr. Housing was maintained at 24°C to 26°C and 50% to 60% relative humidity. After the experiments, the rats were disposed of in accordance with the National Institutes of Health Guidelines for the Care and Use of Laboratory Animals. All protocols used in this study were approved by the Sun Yat-sen University Animal Care and Use Committee.

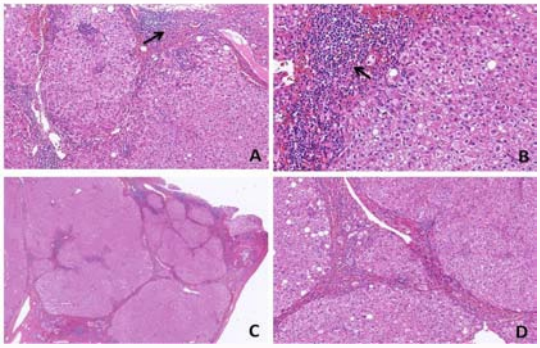

Figure 1: Changes in liver histology in cirrhotic rats. A: Liver cells exhibiting bridging necrosis in the plates of hepatocytes grown within hepatic lobules (HE 10×10). B: Liver cells exhibiting piecemeal necrosis in the plates of hepatocytes grown within hepatic lobules (HE 10×20). C: Normal structures within hepatic lobules were destroyed, and false lobules had formed (HE 2×10). D: Normal structures within hepatic lobules were destroyed, and false lobules had formed (high-power image of an area shown in C, HE 10×10).

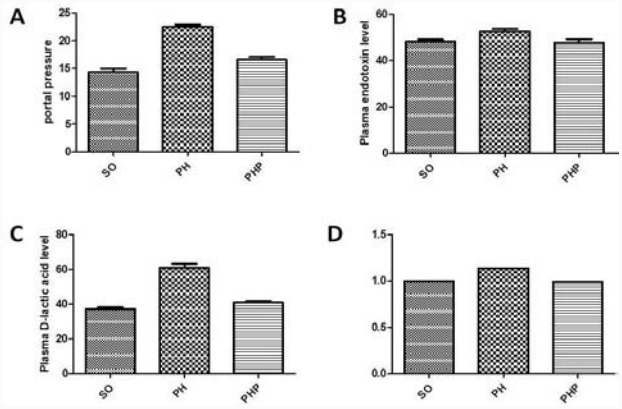

Figure 2: Comparisons of several parameters among three groups. **A**: A comparison of portal pressure among the three groups. Portal pressure was significantly higher in the PH group than in the SO and PHP groups (SO *vs.* PH, P<0.01; PHP *vs.* PH, P<0.01). **B**: **A** comparison of plasma endotoxin levels among the three groups. Plasma endotoxin levels were significantly higher in the rats in the PH group than in those in the SO and PHP groups (P<0.05). **C**: A comparison of plasma D-lactic acid levels among the three groups. Plasma D-lactic acid levels were significantly higher in the rats in the PH group than in the SO and PHP groups (P<0.05). **D**: The total amounts of bacteria in the mesenteric lymph nodes of the three groups. The total quantity of bacteria was 14% higher in the MLNs of the PH group than in those in the SO and PHP groups (P<0.05). There was no significant difference between the PHP and SO groups.

Preparation of animal model

A 40% liquid CCl4 soy bean oil mixture (0.4 ml/100 g body weight) was used to perform abdominal subcutaneous multi-point injections in the rats twice a week. After 10 weeks, 80% of the rats were successfully induced to develop cirrhosis.

Animal groups

A total of 60 cirrhotic rats were randomly divided into Sham Operation (SO), major Hepatectomy (PH) and major Hepatectomy Plus Propranolol (PHP) groups. Each group consisted of 20 rats. A total of 10 rats in each group were selected and measured for portal pressure. The remaining 10 rats were used for detection.

Operation methods and collected materials

The rats were subjected to preoperative fasting for 8 h and provided drinking water ad libitum. Ether was administered intranasally to induce anesthesia, and iodine was used to disinfect the skin in the operation field. A median abdominal incision was performed in the abdomen to expose the liver. In the SO group, the ligament around the liver was cut, and the abdomen was then closed. In the PH group, a modified major hepatectomy was performed on the rats according to the protocol described by Kamada and Andersson [4,5], in which the left inner and outer lobes and the middle lobe were cut from the liver, resulting in a resection of approximately two-thirds of the liver. In the PHP group, a major hepatectomy was conducted, and the rats were then perused with 2 ml of a 5 mg/ml propranolol saline solution at 12 hr and 24 hr after the surgery.

Portal pressure determination

During laparotomy, a small catheter was inserted directly into the portal vein, and portal pressure was measured through a pressure transducer that was connected to a biological signal acquisition system and registered using a multi channel recorder (BL-420F, Chengdu Technology and Market Co., Ltd. Chengdu, China). The results are expressed as cmH_2O.

Materials collected for detection

At 24 h post-operation, the abdomen was re-opened and materials were collected under sterile conditions.

Plasma D-Lactate levels and endotoxin levels

A total of 2 ml of blood was drawn from the inferior vena cava. Plasma was obtained via separation in a centrifuge. The samples were tested with ELISA assays according to the manufacturer's instructions (Shanghai, China, Bio-Techne China Co. Ltd.). D-lactate levels are expressed in mg/L, and endotoxin levels are expressed as EU/ml.

Fecal bacteria detection by PCR

Fecal DNA extraction

Approximately 0.5 g of fecal matter was collected and weighed. A 500 μL volume of protease was added to the samples during lysis, and the solutions were mixed and digested overnight. Tris-balanced phenol chloroform and absolute ethyl alcohol were then used to extract DNA. The program Primer 5.0 was used to design appropriate bacteria genus PCR primers, and the specificity of the primer sequences was compared to the corresponding bacterial sequences in GenBank.

PCR primer design

Enterococcus: F: GGTTTCCGCCCTTCAGTG, R: GAAGCTCTATCTCTAGAGTGGTCA

Clostridium: F: TAATGACGGTACTTTGGAGGA, R: CGTAGCCCTTTCTACCTGC

Bacteroides: F: GCAGCATATTTGTAGCAATACAGAT, R: CTATACCATCGGGTATTAATCTTTC

Bifidobacteria: F: GAGCAAGCCTTCGGGTGAGT, R: GGCCCCACATCCAGCGTC

Colon Bacillus: F: ACGGTAACAGGAAGCAGCTT, R: CCCTCTTTGGTCTTGCGA

Klebsiella pneumonia: F: GATGAAACGACCTGATTGCATTC, R: CCGGGCTGTCGGGATAAG

23S reference: F: AGCGAAAGACAGGTGAGAATCC, R: CCTATCGGCCTCGGCTTAG

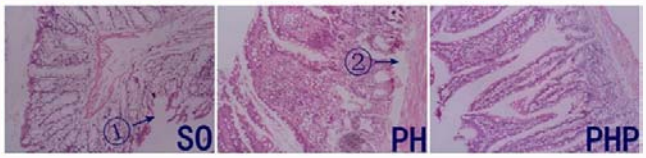

Figure 3: The structure of the intestinal mucosa in the three groups (HE staining). Arrow ① shows that the mucosal epithelium exhibited reduced continuity and shortened intestinal epithelial villi. Arrow ② shows a cracked lamina propria and shrunken intestinal villi. The images were captured at 40× magnification.

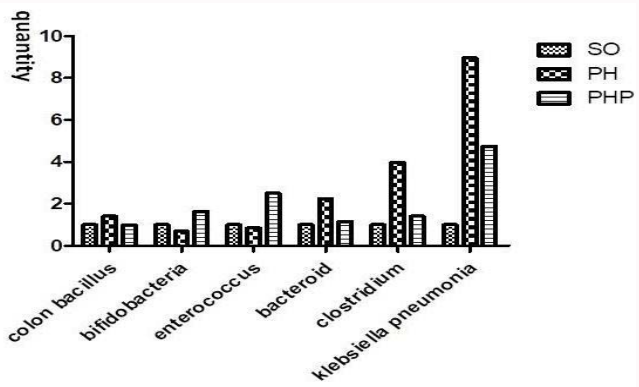

Figure 4: PCR analysis of the composition of fecal bacteria. There were fewer probiotics, such as Bifidobacteria, in the PH group, whereas there were more pathogens, such as colon *Bacillus*, *Bacteroides*, *Clostridium*, and *Klebsiella pneumoniae*.

Fecal bacteria PCR analysis

The amplification system consisted of 0.2 μL of each forward and reverse primer (10 μM), 12.5 μL of Premix Ex Taq™ (2X), 3 μL of template DNA, and enough ddH_2O to reach a final reaction volume of 25 μL. The following PCR conditions were used: one cycle of initial denaturation at 95°C for 15 min followed by 40 cycles of PCR amplification at 94°C for 30 s, 60°C for 30 s, and 72°C for 90 s.

Detection of bacteria in mesenteric lymph nodes

Several Mesenteric Lymph Node (MLN) samples were obtained, and the protocol used to detect bacteria was the same that was used to detect fecal bacteria. The following bacterial primer sequences were used:

F: CTCCTACGGGAGGCAGCAGT and R: ATTACCGCGGCTGCTGGCAC

Small intestine and liver HE staining

The resected distal ileum segments were fixed in neutral-buffered formalin and then processed for histological analysis. The slides were stained with Hematoxylin and Eosin (HE) and analyzed under an optical microscope (Leica DMI4000B) by a single pathologist who was blinded to the sample identities. The pathological changes that occurred in the small intestine mucosa were evaluated using Chiu's scoring method [6]: 0 points, normal; 1 point, the subcutaneous space on the villus tip was widened; 2 points, the subcutaneous space on the villus tip was further expanded, the villus tip epithelium was elevated, and the intrinsic membrane was peeling; 3 points, the villus epithelium was shedding in bulk; 4 points, the epithelium was completely shed, leaving only an inherent film; and 5 points, the inherent film was cracked, and bleeding and ulceration were observed.

Western blot detection of ZO-1 and Claudin-1 in small intestine tissues

Resected distal ileum segments were stored at -80°C. A sample (100 μg) of intestinal mucosal tissue was collected and added to a solution containing lysate and buffer. The mixture was homogenized and centrifuged. The supernatant was collected, and 10 μL of the diluted samples and 5 μL of a prestained marker were loaded onto gels. After denaturation, electrophoresis, film transfer and closure had been performed, the corresponding primary and secondary antibodies were added. GAPDH was used as the inner reference. After the samples were incubated and developed, a quantitative analysis was conducted.

Immunohistochemical detection of TNF-α, IFN-γ and MLCK in small intestine tissues

The distal ileum tissue was collected, embedded, and fixed. Next, the samples were subjected to antigen repair, endogenous peroxidase activity was blocked, and the tissue was incubated with the corresponding primary and secondary antibodies. Subsequently, SABC reagent was added, and the tissues were incubated, colored with DAB, and restrained. In the negative control, the antibody was replaced with PBS. The results of the imunohistochemical analysis were interpreted in semi-quantitative mode using a double-blind method, and cells that appeared as red granules were considered to be positively labeled. Over 75% of the cells that were stained were strongly positive (+++), 50% to 75% were positive (++), 10% to 49% were weakly positive (+), and fewer than 10% were negative.

Statistical analysis

Portal pressure, endotoxin concentration, and D-lactate, ZO-1and Claudin-1 level are expressed as the mean ± standard error, and differences between two groups were analyzed using t-tests for two independent samples. The results of PCR to detect fecal components and MLN bacteria were analyzed using a gene/inner reference gene method for the expression level analysis. We used Chiu's scoring system for small intestine tissue samples to compare the two groups of independent samples (i.e., the Wilcoxon test). The results of immunohistochemistry in the ileum for TNF-α, IFN-γ and MLCK showed that they were expressed at a strong positive rate, and Pearson's $\chi 2$ test was used to analyze the detection data. $P<0.05$ indicated a significant difference.

Results

Histological changes in the liver

In the 6th week, liver cells exhibited piecemeal (Figure 1A) and bridging necrosis (Figure 1B) in plates of hepatocytes grown within hepatic lobules. After 10 weeks, the liver cells were arranged in a disorderly fashion. The normal structures of the hepatic lobules were destroyed, and false lobules had formed (Figure 1C, 1D). Slight bile duct proliferation and extensive fibrous tissue proliferation were also observed.

Portal pressure

Portal pressure was 14.3 ± 1.25 cmH_2O in the SO group. It was significantly higher in the PH group (22.48 ± 0.882 cm H2O, $P<0.01$) than in the SO group and significantly lower in the PHP group (16.6 ± 1.02 cmH_2O, $P<0.01$) than in the PH group (Figure 2A).

Plasma endotoxin and D-lactic acid levels

The plasma endotoxin and D-lactic acid levels in the SO group were 48.28 ± 1.45 EU/ml and 37.23 ± 1.71 mg/L, respectively. In the

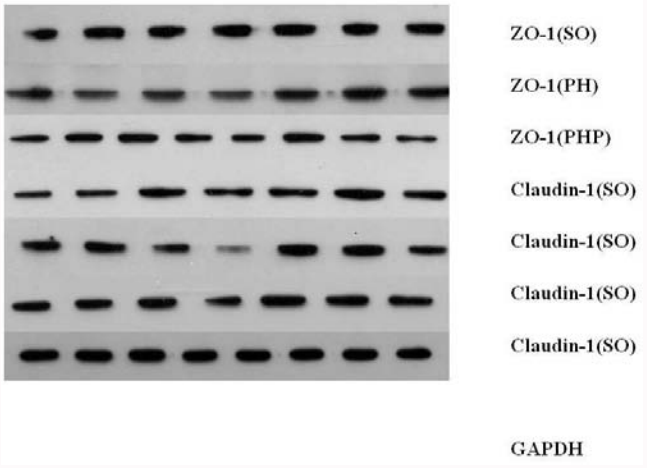

Figure 5: Western blots used to detect the ZO-1 and Claudin-1 proteins. Western blot assays showed that the expression levels of the ZO-1 and Claudin-1 proteins was significantly lower in the PH group than in the SO and PHP groups. There was no significant difference between the SO and PHP groups.

PH group, the levels were higher, at 52.56 ± 2.08 EU/ml (SO *vs.* PH, P<0.05) and 60.87 ± 4.44 mg/L (SO *vs.* PH, P<0.05), respectively. However, plasma endotoxin and plasma D-lactic acid levels were lower in the PHP group than in the PH group (47.84 ± 3.45 *vs.* 52.56 ± 2.08EU/ml and 40.83 ± 1.82 *vs.* 60.87 ± 4.44 mg/L, respectively; P<0.01 for both), and this difference was associated with a lower prevalence of BT (Figure 2B, 2C).

PCR detection of MLN bacteria

The total amount of bacteria in the MLNs was 14% higher in the PH group than in the SO and PHP groups (P<0.05), although there was no significant difference between the PHP and SO groups (Figure 2D).

Small intestine pathology according to the Chiu score

The structure of the intestinal mucosa was generally normal in the SO group, although there was less continuity in the mucosal epithelium and shortened intestinal epithelial villi. Above the villus, the subcutaneous space had widened, the intestinal villus tip epithelium was elevated, and the fixed film had peeled. The continuity of the intestinal mucosa was relatively poor in the PH group, in which the intestinal mucosa epithelium was shedding in bulk and in some places even completely falling off. The fixed layer was cracked, and its intestinal villus was smaller than that observed in the SO group. The Chiu scores showed that the average score for rat mucosal damage was significantly higher in the PH group (22.55) than in the SO group (7.35). The score for the structure of the intestinal mucosa in the PHP group was 16.6, which was between the scores for the PH and SO groups described above (PHP *vs.* PH, P<0.05) (Figure 3).

PCR analysis of fecal bacteria

The amounts of fecal *Clostridium* and *Bacteroides* and colon *Bacillus* species were 125%, 297% and 796% higher, respectively, while the amounts of *Bifidobacteria* and *Enterococcus* species were 31% and 15% lower, respectively, in the PH group than in the fecal samples obtained in the SO group. However, the amounts of fecal *Clostridium*, *Bacteroides* and colon *Bacillus* were significantly lower and the amounts of *Bifidobacterium* and *Enterococcus* were significantly higher in the PHP group (P<0.05) (Figure 4).

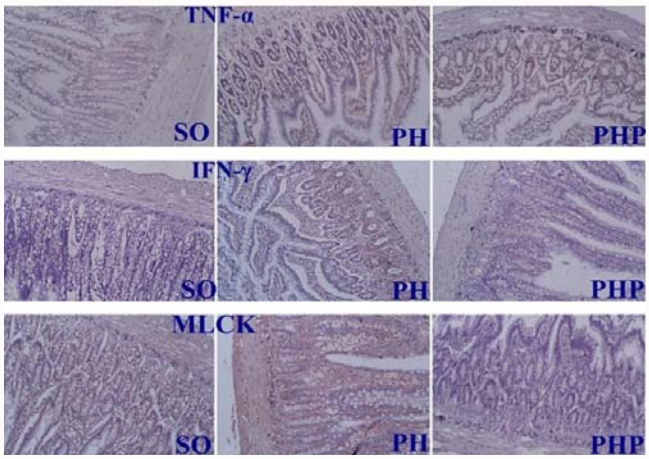

Figure 6: Immunohistochemical study of the intestinal mucosa. Cells showing positive expression (red granules) were observed. The proportions of cells that were strongly positive for TNF-α, IFN-γ and MLCK expression were significantly higher in the PH group than in the SO and PHP groups.

Western blot assay

Western blot assays showed that the expression levels of the ZO-1 and Claudin-1 proteins were significantly lower in the PH group than in the SO and PHP groups, although there were no significant differences in these levels between the SO and PHP groups (Figure 5).

Immunohistochemical study of the intestinal mucosa

When TNF-α, IFN-γ and MLCK were detected in small intestine tissues, cells with the appearance of red granules were observed. The proportions of positive cells were different among three groups. The proportions of cells that strongly expressed TNF-α, IFN-γ and MLCK were significantly higher in the PH group (40%, 50%, 70%) than in the SO (20%, 10%, 20%) and PHP (30%, 20%, 40%) groups (P<0.05; Figure 6).

Discussion

Intestinal bacterial translocation is one of the causes of postoperative infection after major hepatectomy [7]. Many underlying factors affect how much translocation occurs, including the reticuloendothelial system [8], which reduces damage to the intestinal mechanical, bacterial and immune barriers [9-11], increases in the levels of intestinal tissue inflammatory factors [12], and intestinal ischemia reperfusion injury [13]. The mechanical barriers presents the most important barrier in the intestines, and its structure is closely associated with the expression of members of the ZO and Claudin families of proteins [14,15]. In the present study, Western blot analysis revealed that the expression levels of ZO-1 and Claudin-1 were significantly lower in the PH group than in the SO and PHP groups. In addition, the plasma levels of D-lactic acid and endotoxin and the amount of bacteria in the MLNs were significantly higher in the PH group than in the other groups, indicating that the structure of the intestines was tightly associated with the amount of damage that was observed. Intestinal permeability was increased, and intestinal bacteria and their products had penetrated the intestinal epithelium and entered MLNs. This allowed them to invade other tissues and organs, resulting in postoperative infection. This process therefore represents one of the mechanisms by which bacterial translocation can occur after major hepatectomy. The decreases in the expression of ZO-1 and Claudin-1 that were observed in the cirrhotic rats after major hepatectomy may have resulted from the following

underlying causes. a) An increase in portal pressure, which occurs after major hepatectomy, causes the intestinal mucosa to exist in a state of low perfusion. Intestinal epithelial cells therefore reside in a state of severe hypoxia, leading to a locally harmful accumulation of metabolites, which causes acidosis and stimulates the adherence, aggregation and activation of white blood cells. These changes were followed by the release of kinins, oxygen-free radicals, proteases, and lysosomal enzymes. These factors cause the lipids in the cell and mitochondrial membranes to undergo peroxidation and calcium overload reactions, which eventually lead to cell death or epithelial apoptosis. b) Increases in inflammatory factors may be involved because the results of the present study show that the proportions of cells that are strongly positive for TNF-α and IFN-γ expression were significantly higher in the PH group than in the SO and PHP groups. TNF-α is an important regulatory factor of intestinal mechanical barrier function. A previous study showed that TNF-α induces intestinal epithelial cells to undergo bulk shedding [16]. TNF-α up-regulates the expression of MLCK, as confirmed by our results [17-19]. TNF-α induces NF-κB to translocate to the nucleus from the cytosol, and factors downstream of TNF-α are then activated, resulting in the promotion of apoptosis-related genes, such as Fas/FasL genes, and the induction of epithelial cell apoptosis [20]. An increase in TNF-α level can directly inhibit the expression of ZO-1 transcription [21]. IFN-γ promotes micropinocytosis in epithelial cells, which results in the promotion of Claudin and Occlud in activity and the subsequent failure of tight junction integrity [22]. c) Endotoxin-damaged mitochondria and lysosomes were observed in intestinal epithelial cells, and ischemia and hypoxia resulted in shrinkage of intestinal vessels [23]. We found that endotoxin shad translocated and entered the liver, where they stimulated Kupffer cells to secrete a variety of inflammatory factors, resulting in a continuous increase in the levels of inflammatory factors in the blood, which caused damage to the intestinal mucosa [21]. d) MLCK expression was up-regulated. Myosin undergoes conformational changes when phosphorylated, resulting in the contraction of the actin skeleton and leading to barrier dysfunction in the intestinal epithelium. In addition, MLCK promotes the endocytosis of Occlud in [18,19] in intestinal epithelial cells in response to inflammatory mediators, such as TNF-α. e) Liver resection may have contributed to the changes observed in their expression. After hepatectomy, the number of cells in the reticuloendothelial system and the number of Kupffer cells in the liver were significantly lower. The rate of hepatic clearance of endotoxins and bacteria from the abdominal cavity decreased in the liver, resulting in endotoxemia and bacteremia, which in turn increased intestinal tight junction damage. The intestinal microbial ecosystem plays an important role in the immune system and the maturation of other physiological processes [24,25]. Under normal circumstances, various bacteria exist in a dynamic equilibrium that constitutes the intestinal biological barrier. In the present study, the mechanism underlying intestinal bacterial translocation was associated with changes in the composition of fecal bacteria and involved the following processes. a) Probiotic antagonistic effects reduced pathogen colonization. Probiotics can produce short-chain fatty acids that reduce intestinal PH and promote the secretion of antimicrobial peptides [26]. The results of the present study show that the amount of *Bifidobacteria* in the PH group was only 69% of the amount observed in the SO group. This difference benefited the reproduction of the pathogen *Escherichia coli* and promoted damage to the intestinal epithelium [27]. In addition, probiotic products, such as butyric acid, can up-regulate intestinal epithelial cells via the antibacterial peptide LL-37, provide energy for intestinal epithelial cells, and promote the proliferation and repair of epithelial cells [28]. b) The levels of intestinal tight junction proteins were decreased. Probiotics can up-regulate the expression of Claudin-1 and Occludin-1, resulting in improved colonic permeability [29], and inhibiting the expression of these proteins increases intestinal permeability. Additionally, decreasing the amount of *Bifidobacteria* increased cell membrane wrinkling by colonic epithelial cells and down-regulated ZO-1 expression [30]. c) Intestinal pathogenic bacteria were increased. There was a significant increase in intestinal pathogenic bacteria in the PH group (i.e., *Escherichia coli*, *Clostridium*, *Klebsiella*, and *Bacteroides*). When intestinal bleeding occurs, *Escherichia coli* and *Clostridium welchii* can directly damage or induce the phosphorylation and dephosphorylation of closely connected structural proteins, resulting in the redistribution of tight connection structures between the cell membrane and cytoplasm and damaging their integrity [31]. d) Nutrient competition is affected, in that probiotics reside in the human intestine, and probiotics are better than pathogens at adapting to the intestinal environment, and they show stronger survival skills and are better able to compete for nutrients, which allows them to inhibit the growth of pathogenic bacteria. In the present study, the number of postoperative probiotics was lower, and the proportion of pathogenic bacteria was higher, and these effects weakened the competitive ability of the probiotic nutrients and caused the proportions of maladjusted bacterial groups to continuously increase. e) A reduction in intestinal probiotics damages the function of the intestinal immune system. Unique types of bacteria that reside in the intestinal lumen have been shown to adhere to the intestinal Peyer's lymph nodes in rats and to strongly stimulate regulatory T cells in the lamina propria, resulting in an increase in the number of T cell subsets and there by contributing to resistance in pathogen colonies and stimulating the secretion of intestinal S-IgA [32,33]. f) Overgrowth of pathogenic bacteria directly damages intestinal epithelial cells. The bacterial proteases that are secreted by overgrown pathogenic bacteria were found to damage microvilli by directly damaging microvilli membrane proteins in intestinal epithelial cells [34].

The results of the present study show that after hepatectomy was performed in cirrhotic rats, portal pressure increased, and the levels of the inflammatory factors TNF-α and IFN-γ and the enzyme MLCK were increased, resulting in damage to the intestinal mechanical barrier. Additionally, in the rats that underwent surgery, the expression of the ileal structural proteins ZO-1 and Claudin-1 was lower, the composition of the intestinal bacteria was altered, the proportions of probiotics were lower, the proportions of pathogens were higher, and intestinal permeability had increased. The intestinal mechanical and bacterial barriers were both damaged, and these effects represent one of the mechanisms by which bacterial translocation can occur after major hepatectomy. Propranolol can reduce portal pressure and intestinal congestion, resulting in a reduction in damage to the intestinal mucosal barrier, reducing endotoxemia, restoring balance to and the maintenance of intestinal bacteria and reducing damage to the intestinal mechanical barrier. Each of these effects may effectively reduce bacterial translocation in the intestines.

Acknowledgement

This work was supported by the National Natural Science Foundation of China (grant number 81172783).

References

1. Uchiyama K, Ueno M, Ozawa S, Kiriyama S, Kawai M, Hirono S, et al. Risk factors for postoperative infectious complications after hepatectomy. J Hepatobiliary Pancreat Sci. 2011;18(1):67-73.
2. Capussotti L, Viganò L, Giuliante F, Ferrero A, Giovannini I, Nuzzo G. Liver dysfunction and sepsis determine operative mortality after liver resection. Br J Surg. 2009;96(1):88-94.
3. Chen WZ, Hu KP, Xu RY, Pan WD. Beneficial effect of splenic artery ligation on bacterial translocation after major liver resection in rats. Dig Liver Dis. 2013;45(3):233–7.
4. Ekberg H, Tranberg KG, Andersson R, Jeppsson B, Bengmark S. Major liver resection: perioperative course and management. Surgery. 1986;100(1):1-8.
5. Kamada N, Calne RY. A surgical experience with five hundred thirty liver transplants in the rat. Surgery. 1983;93:64-69.
6. Chiu CJ, McArdle AH, Brown R, Scott HJ, Gurd FN. Intestinal mucosal lesion in low-flow states. I. A morphological, hemodynamic, and metabolic reappraisal. Arch Surg. 1970;101(4):478-83.
7. Wang X, Andersson R, Soltesz V, Bengmark S. Bacterial translocation after major hepatectomy in patients and rats. Arch Surg. 1992;127(9):1101-6.
8. Wang XD, Pärsson H, Andersson R, Soltesz V, Johansson K, Bengmark S. Bacterial translocation, intestinal ultrastructure and cell membrane permeability early after major liver resection in the rat. Br J Surg. 1994;81(4):579-84.
9. Nakao T, Kurita N, Komatsu M, Yoshikawa K, Iwata T, Utusnomiya T, et al. Irinotecan injures tight junction and causes bacterial translocation in rat. J Surg Res. 2012;173(2):341-7.
10. Benten D, Wiest R. Gut microbiome and intestinal barrier failure--the "Achilles heel" in hepatology? J Hepatol. 2012;56(6):1221-3.
11. McGhee JR, Fujihashi K. Inside the mucosal immune system. PLOS Biology. 2012.
12. Watson AJ, Hughes KR. TNF-α-induced intestinal epithelial cell shedding: implications for intestinal barrier function. Ann N Y Acad Sci. 2012;1258:1-8.
13. Nakagawa H, Tsunooka N, Yamamoto Y, Yoshida M, Nakata T, Kawachi K. Intestinal ischemia/reperfusion-induced bacterial translocation and lung injury in atherosclerotic rats with hypoadiponectinemia. Surgery. 2009;145(1):48-56.
14. Van Itallie CM, Anderson JM. Claudins and epithelial paracellular transport. Annu Rev Physiol. 2006;68:403-29.
15. Fasano A. Zonulin and its regulation of intestinal barrier function: the biological door to inflammation, autoimmunity, and cancer. Physiol Rev. 2011;91(1):151-75.
16. Kiesslich R, Duckworth CA, Moussata D, Gloeckner A, Lim LG, Goetz M, et al. Local barrier dysfunction identified by confocal laser endomicroscopy predicts relapse in inflammatory bowel disease. Gut. 2012;61(8):1146-53.
17. Ye D, Ma I, Ma TY. Molecular mechanism of tumor necrosis factor—a modulation of intestinal epithelial tight junction barrier. Am J Physiol Gastrointest Liver Physiol. 2006;290(3):G496-504.
18. Shen L, Turner JR. Role of epithelial cells in initiation and propagation of intestinal inflammation. Eliminating the static: tight junction dynamics exposed. Am J Physiol Gastrointest Liver Physiol. 2006;290(4):G577-82.
19. Utech M, Mennigen R, Bruewer M. Endocytosis and recycling of tight junction proteins in inflammation. J Biomed Biotechnol. 2010;2010:484987.
20. Campbell KJ, Rocha S, Perkins ND. Active repression of antiapoptotic gene expression by RelA(p65) NF-kappa B. Mol Cell. 2004;13(6):853-65.
21. Song HL, Lv S, Liu P. The roles of tumor necrosis factor-alpha in colon tight junction protein expression and intestinal mucosa structure in a mouse model of acute liver failure. BMC Gastroenterol. 2009;22:70.
22. Bruewer M, Utech M, Ivanov AI, Hopkins AM, Parkos CA, Nusrat A. Interferon-gamma induces internalization of epithelial tight junction proteins via a macropinocytosis-like process. FASEB J. 2005;19(8):923-33.
23. Catalioto RM, Maggi CA, Giuliani S. Intestinal epithelial barrier dysfunction in disease and possible therapeutical interventions. Curr Med Chem. 2011;18(3):398-426.
24. Smith K, McCoy KD, Macpherson AJ. Use of axenic animals in studying the adaptation of mammals to their commensal intestinal microbiota. Semin Immunol. 2007;19(2):59-69.
25. Hooper LV, Wong MH, Thelin A, Hansson L, Falk PG, Gordon JI. Molecular analysis of commensal host-microbial relationships in the intestine. Science. 2001;291(5505):881-4.
26. Lupp C, Robertson ML, Wickham ME, Sekirov I, Champion OL, Gaynor EC, et al. Host-mediated inflammation disrupts the intestinal microbiota and promotes the overgrowth of Enterobacteriaceae. Cell Host Microbe. 2007;2(2):119-29.
27. Keeney KM, Finlay BB. Enteric pathogen exploitation of the microbiota-generated nutrient environment of the gut. Curr Opin Microbiol. 2011;14(1):92-8.
28. Maslowski KM, Vieira AT, Ng A, Kranich J, Sierro F, Yu D, et al. Regulation of inflammatory responses by gut microbiota and chemoattractant receptor GPR43. Nature. 2009;461(7268):1282-6.
29. Corridoni D, Pastorelli L, Mattioli B, Locovei S, Ishikawa D, Arseneau KO, et al. Probiotic bacteria regulate intestinal epithelial permeability in experimental ileitis by a TNF-dependent mechanism. PLOS ONE. 2012;7:0042067.
30. Jones SE, Versalovic J. Probiotic Lactobacillus reuteri biofilms produce antimicrobial and anti-inflammatory factors. BMC Microbiol. 2009;9:35.
31. Simonovic I, Rosenberg J, Koutsouris A, Hecht G. Enteropathogenic Escherichia coli dephosphorylates and dissociates occludin from intestinal epithelial tight junctions. Cell Microbiol. 2000;2(4):305-15.
32. Gaboriau-Routhiau V, Rakotobe S, Lécuyer E, Mulder I, Lan A, Bridonneau C, et al. The key role of segmented filamentous bacteria in the coordinated maturation of gut helper T cell responses. Immunity. 2009;31(4):677-89.
33. Lara-Villoslada F, Sierra S, Boza J, Xaus J, Olivares M. Beneficial effects of consumption of a dairy product containing two probiotic strains, Lactobacillus coryniformis CECT5711 and Lactobacillus gasseri CECT5714 in healthy children. Nutr Hosp. 2007;22(4):496-502.
34. Barber AE, Jones WG, Minei JP, Fahey TJ, Lowry SF, Shires GT. Bacterial over growth and intestinal at rophy in the etiology of gut barrier failure in the rat. Am J Surg. 1991;161(2):300-4.